Generation and structure of extremely large clusters in pulsed jets

Daniela Rupp, Marcus Adolph, Leonie Flückiger, Tais Gorkhover, Jan Philippe Müller, Maria Müller, Mario Sauppe, David Wolter, Sebastian Schorb, Rolf Treusch, Christoph Bostedt, and Thomas Möller

Citation: The Journal of Chemical Physics **141**, 044306 (2014); doi: 10.1063/1.4890323
View online: http://dx.doi.org/10.1063/1.4890323
View Table of Contents: http://scitation.aip.org/content/aip/journal/jcp/141/4?ver=pdfcov
Published by the AIP Publishing

Generation and structure of extremely large clusters in pulsed jets

Daniela Rupp,[1,a)] Marcus Adolph,[1] Leonie Flückiger,[1] Tais Gorkhover,[1,2] Jan Philippe Müller,[1] Maria Müller,[1] Mario Sauppe,[1] David Wolter,[1] Sebastian Schorb,[1,2] Rolf Treusch,[3] Christoph Bostedt,[2,4] and Thomas Möller[1]

[1]*IOAP, Technische Universität Berlin, Hardenbergstraße 36, 10623 Berlin, Germany*
[2]*Linac Coherent Light Source, SLAC National Accelerator Laboratory, 2575 Sand Hill Road, Menlo Park, California 94025, USA*
[3]*FLASH, DESY, Notkestraße 85, 22603 Hamburg, Germany*
[4]*PULSE Institute, Stanford University and SLAC National Accelerator Laboratory, 2575 Sand Hill Road, Menlo Park, California 94025, USA*

(Received 19 May 2014; accepted 18 June 2014; published online 25 July 2014)

Extremely large xenon clusters with sizes exceeding the predictions of the Hagena scaling law by several orders of magnitude are shown to be produced in pulsed gas jets. The cluster sizes are determined using single-shot single-particle imaging experiments with short-wavelength light pulses from the free-electron laser in Hamburg (FLASH). Scanning the time delay between the pulsed cluster source and the intense femtosecond x-ray pulses first shows a main plateau with size distributions in line with the scaling laws, which is followed by an after-pulse of giant clusters. For the extremely large clusters with radii of several hundred nanometers the x-ray scattering patterns indicate a grainy substructure of the particles, suggesting that they grow by cluster coagulation. © *2014 AIP Publishing LLC*. [http://dx.doi.org/10.1063/1.4890323]

I. INTRODUCTION

Gas phase clusters have become a system of choice for studying the interaction of intense radiation with matter as they are intermediate to atomic systems and the solid state regime.[1–7] Specifically rare gas clusters from a supersonic gas expansion are commonly used because they are easy to produce and tunable in size by changing either gas pressure or temperature.[8] Semi-empirical scaling laws for calculating average cluster sizes in cw gas jets have been derived decades ago by Hagena and others[9–12] using Rayleigh and He scattering and mass spectrometry.

In numerous of today's applications it is more efficient to use pulsed valves instead of cw-jets in order to match the cluster production gas load with the repetition rate of the high power laser sources. Further, some experiments require the use of cluster sizes in excess of the available parameter space of the scaling laws.[5] Common strategies to produce very large clusters in a gas expansion cause experimental problems because high stagnation pressure and large nozzle diameters induce a very high gas load even with pulsed sources. In addition, the use of very low temperatures in the vicinity of the vapor pressure curve increases the danger of freezing the nozzle.

In this article we describe a new method for generating extremely large clusters with a pulsed source. We have analyzed the time structure of a pulsed supersonic cluster jet by means of single particle imaging with intense x-ray pulses from the free-electron laser in Hamburg (FLASH).[13] We find that the main cluster pulse is followed by an after-pulse of extremely large clusters, exceeding the predictions of the scaling laws by several orders of magnitude. The discovery and characterization of these μm-clusters after the pulse gives access to a new regime of studies on laser-cluster interaction while maintaining low gas loads even in high repetition-rate experiments.

II. EXPERIMENTAL DETAILS

The overall setup is shown in Figure 1 (similar to a previous experiment[4]). Xenon clusters were produced by supersonic expansion of gas through a cryogenically cooled, conical nozzle (Ø200 μm, 4° half opening angle) mounted on a solenoid valve.[14] For opening the valve and allowing for gas flow, a Vespel poppet in a ferromagnetic holder was pulled back by the solenoid against the force of a spring, and released again for closing.

We used xenon as sample material since it has a high binding energy and therefore allows for the production of large clusters. Temperature and stagnation pressure of the gas were varied to explore different expansion regimes and obtain a large range of different cluster sizes. The size and particle morphology were characterized in single-shot single-particle scattering experiments at the FLASH free-electron laser. FLASH delivers $\sim 10^{13}$ soft x-ray photons in a single pulse of about 100 fs duration,[15] allowing for recording scattering patterns of individual clusters in single shots.

The experiment was carried out at 92 eV photon energy within the giant resonance of xenon, i.e., at a large scattering efficiency. The xenon cluster beam was guided into the main chamber through two differentially pumped conical skimmers and spatially overlapped with the focused FEL beam. Overlap and focal position could be optimized with an ion time-of-flight mass spectrometer (similar geometry as in Ref. 16).

a)Electronic mail: daniela.rupp@physik.tu-berlin.de

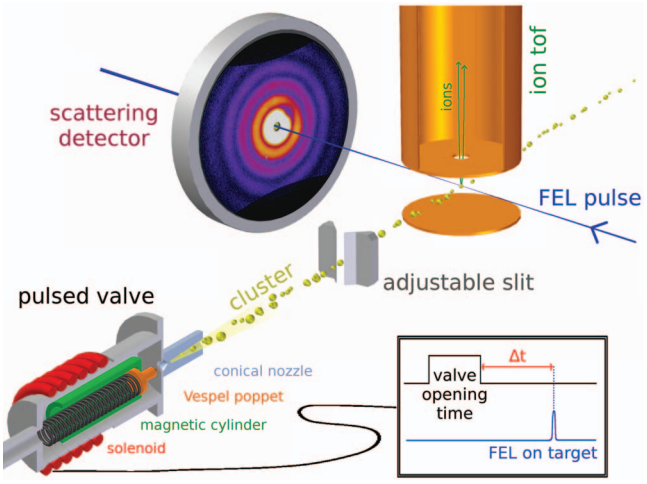

FIG. 1. Schematic setup for analyzing a pulsed supersonic jet with single-shot single-cluster imaging. For cluster generation a solenoid driven valve releases a gas pulse through a conical nozzle into vacuum. The time delay between cluster pulse and FEL pulse was scanned to map the cluster size distributions along the cluster pulse. See text for further explanation.

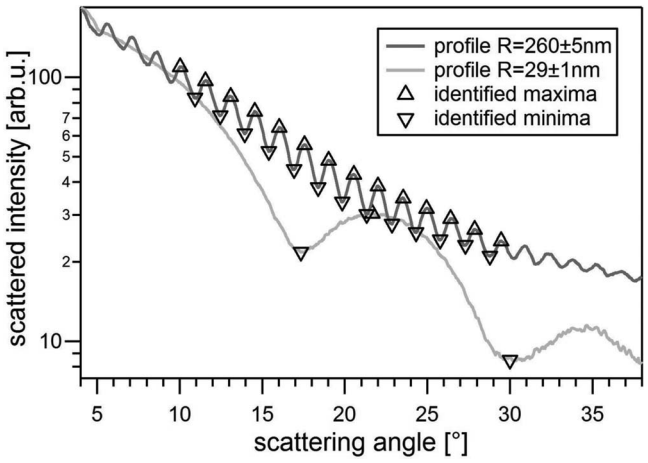

FIG. 2. Two examples for deriving the cluster size from single-cluster scattering images. A segment of the scattering detector is radially averaged. These scattering profiles are automatically analyzed for maxima and minima. Positions and spacing of the minima are compared to Mie simulations to obtain the cluster size.

The pulsed valve was opened for 5 ms at a rate of 5 Hz, matching the repetition rate of the FEL pulses. The synchronization, i.e., time delay between cluster pulse and FEL pulse was scanned to map the cluster size distributions along the cluster pulse. The number of clusters in the interaction volume could be varied by a piezoelectric driven skimmer slit with an adjustable width between 0 and 1.5 mm. For measurements on individual clusters it was closed until most recorded images were dark and the interjacent bright patterns typically showed a single cluster in the focal volume.

The scattering patterns were detected with a large-area detector at 47 mm distance to the interaction region. The photon signal was amplified by an MCP with 75 mm active area and converted into visible photons by a phosphor screen. The resulting scattering angles range from 4° to 38°, corresponding to a maximal momentum transfer of 0.30 nm^{-1} and a resolution of 23 nm, respectively (cf. Ref. 17). The visible image on the screen was recorded shot-to-shot with an out-of-vacuum CCD camera (not in Fig. 1, cf. Ref. 5). All parts of the scattering detector system exhibit a hole in the center to release the primary FEL beam out of the interaction region.

The size of each cluster was determined by analyzing the radial profile of each single pattern as exemplified in Figure 2. Therefore, an azimuthal segment of about 80° on the right side of the scattering pattern[18] was radially averaged and maxima and minima were automatically identified and fitted with Mie's theory (cf. Ref. 5). Only cluster sizes between 15 nm and 700 nm radius could be analyzed within the current setup. Smaller clusters did not show a clear minimum on the detector (first minimum for $r = 15$ nm at 35°) and larger clusters than $r = 700$ nm could not be clearly identified because the increasingly fine interference rings became irresolvable.

III. SIZE DISTRIBUTIONS DURING AND AFTER VALVE OPENING

In our experiments we were able to produce giant clusters with radii of several hundreds of nanometers in two different ways:

- We found them in the *main cluster pulse* during the opening of the solenoid valve. Xenon was expanded from initial conditions above the vapor pressure curve where the nozzle was close to clogging due to freezing. Giant clusters appeared with very low statistics as the "large limit" of a distribution of typically much smaller clusters.
- We identified an *after-pulse* of exclusively large clusters when the main pulse was already over, even at much more relaxed expansion conditions.

Stagnation pressure and nozzle temperature for all expansion conditions studied in this work are plotted in Figure 3 within the phase diagram of xenon (data from Ref. 19). Cases A to D from far below to significantly above the vapor pressure curve are discussed in detail in the following paragraphs.

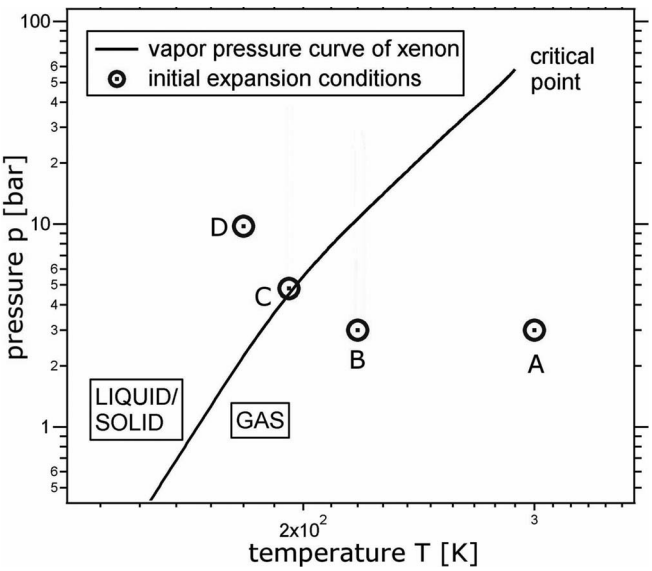

FIG. 3. Phase diagram with vapor pressure curve of xenon (data from Ref. 19). The different expansion settings used in this experiment are denoted as A, B, C, and D.

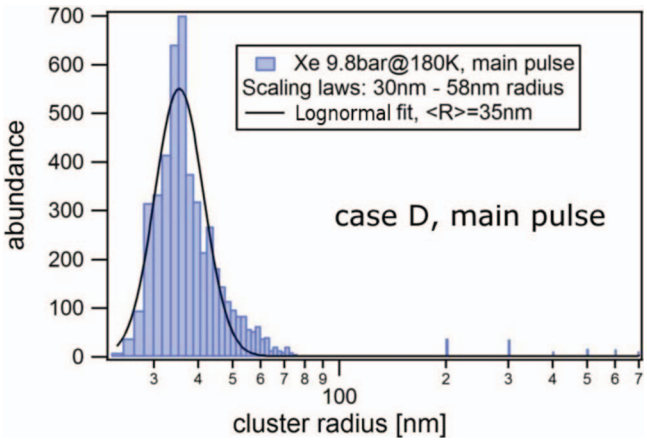

FIG. 4. Size distribution *in the main pulse* for case D, expansion from liquid phase. Scaling laws for the expansion of gas predict sizes between 30 and 58 nm radius,[9,12] see text for further explanation. The experimentally obtained radii are distributed around 35 nm. Note that a few giant clusters from 200 to >700 nm radius were produced.

The expansion condition to be investigated for the cluster size distribution in the *main pulse* is point D, with a stagnation pressure of 9.8 bars and a nozzle temperature of T=180 K residing considerably above the vapor pressure curve. This is where one intuitively expects the generation of the largest clusters but as shown later the time structure of the pulse plays an even more important role. The timing of the source valve relative to the FEL pulse was put to typical conditions[21] of pulsed supersonic expansion measurements: The FEL intercepted the cluster pulse 3 ms after the valve opening, at about two thirds of the valve opening period of 5 ms. As the cluster density during the main pulse is high, the adjustable skimmer slit had to be closed until single-cluster-conditions were achieved. Figure 4 displays the distribution of cluster sizes found in this measurement. A lognormal fit of the size distribution indicates an average cluster size of $r = 35$ nm corresponding to 3×10^6 atoms per cluster. Hagena's law[9] predicts an average radius of 58 nm ($\widehat{=}1 \times 10^7$ atoms per cluster) for those conditions, which slightly overestimates the experimental results. The extension of the scaling laws for larger clusters introduced by Dorchies[12] however delivers a value of $r = 30$ nm ($\widehat{=}2 \times 10^6$ atoms per cluster). Considering the fact that both scaling laws only apply to the expansion of gas, not from the liquid regime, the agreement is surprisingly good.

Very few giant ($r = 200$–700 nm) clusters were found in the single shot data in the tail of the size distribution. In order to make them more visible, the histogram and fit curve in Figure 4 were plotted semi-logarithmically and radii bigger than 150 nm were combined to hundreds. Expanding xenon from above the vapor pressure curve thus produces a small amount of giant clusters but as a method it has several disadvantages. In conventional gas-phase cluster experiments on ensembles of clusters the giant clusters would be buried under the signal of the main distribution. Also single-cluster applications aiming for large clusters would suffer under bad statistics, an extremely high gas load and very unstable expansion conditions as the nozzle might freeze.

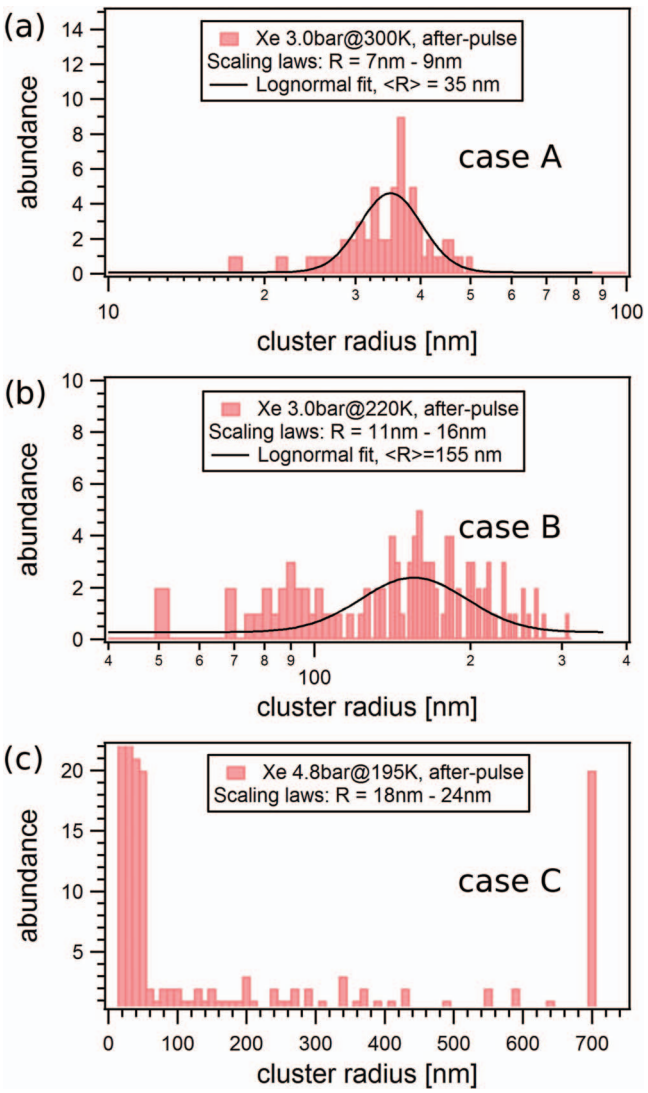

FIG. 5. Cluster size distributions *in the after-pulse* for cases A, B, and C. The size distributions in the after-pulses in (a) and (b) can be fitted by lognormal curves. The histogram in (c) reveals radii from 15 to >700 nm without exhibiting a central maximum. The large number of medium sized clusters below 50 nm radius might originate from a late part of the main pulse, which contains already resolvable cluster sizes. Scattering patterns with cluster radii of 700 nm and larger were all binned into the last peak.

The second way of producing giant clusters in an *after-pulse* at more relaxed expansion conditions below and on the vapor pressure curve (cases A–C in Fig. 3) is much more interesting from this point of view. By scanning the synchronization time between valve opening and FEL trigger we found unexpectedly large clusters after the main cluster pulse, delayed by up to several milliseconds. Figure 5 shows the size distributions found for the expansion conditions A, B, and C between 2 and 9 ms *after the valve was closed*. The data sets were all taken with a fully open skimmer slit since the cluster density in the after-pulses is small anyway. Therefore, the data sets are in the single-cluster limit revealing only extremely large clusters in a rather small size distribution (cf. lognormal fits in Figs. 5(a)) and 5(b)).[20] The predicted cluster sizes in the main pulse and the experimentally obtained average radii are compared in Table I. The measured average radii in the

TABLE I. Cluster sizes measured in the after pulse compared to calculated sizes from scaling laws.[12]

	A	B	C
Experiment: $R_{after-pulse}$	35 nm	155 nm	...
Experiment: atoms/cluster	3×10^6	3×10^8	...
Prediction:[12] $R_{main\,pulse}$	7 nm	11 nm	18 nm
Prediction:[12] atoms/cluster	3×10^4	1×10^5	4×10^5

after-pulse (cf. Figs. 5(a) and 5(b)) exceed the predicted values by factors 5 (case A) and 14 (case B), respectively. In terms of atoms per cluster, the clusters in the after-pulses are 100 and 1800 times bigger than the scaling laws predict.

Also more extreme expansion conditions located on the vapor pressure curve (case C in Fig. 3, 4.8 bars xenon at 195 K) reveal an after-pulse of extremely large clusters reaching and exceeding the resolution limit of 700 nm radius. But as displayed in Figure 5(c)), the obtained size distribution is less defined—the reason might be a superposition of medium sized clusters from the main pulse. Therefore, a reasonable comparison between experimentally obtained and predicted size cannot be given for case C. However, the clusters in the after-pulse are orders of magnitude bigger than predicted: a xenon cluster with radius 700 nm contains 2×10^{10} atoms, about a factor of 5×10^4 more than estimated with Dorchies' law.[12]

IV. TIME STRUCTURE OF A PULSED CLUSTER JET

This interesting and unexpected temporal structure of the pulsed jet was analyzed in more detail for cases A and B. The scattering signal for case A, integrated over the detector area and averaged over 100 FEL pulses for every delay, is plotted versus valve trigger delay in the uppermost panel of Figure 6. The time structure of a pulsed jet can be nicely exemplified here as the different domains are well separated. An about 6 ms wide plateau from 0.5 to 6.5 ms is labeled "scaling laws"-domain because the single-shot data contain only bright patterns of many small clusters as expected from the scaling laws.[12] It is followed by an after-pulse of large clusters around 8 ms, denoted as "XL" (extremely large). In the XL-domain the single shot data reveal that most patterns are dark and only few, very bright patterns show single large clusters. From 9 to 10 ms a second domain appears with all bright, unstructured scattering patterns, which is again followed by a second after pulse of few single large clusters. Case B, plotted in the middle panel of Figure 6, follows a similar sequence but the different domains appear to overlap.

In order to disentangle cluster-related effects and artifacts of the used valve, an additional delay scan was taken with atomic gas, which is displayed in the bottom panel of Figure 6. Here, the integrated ion signal is plotted versus valve trigger delay.[22] Also in the atomic jet a plateau-like structure appears between 0.5 and 6.5 ms. This plateau is followed by a second peak around 9 ms which indicates a second valve opening, maybe due to a rebounce of the poppet which is pushed towards the nozzle by a spring (cf. Fig. 1). This second valve opening is an artifact of our valve, but in fact it helps to

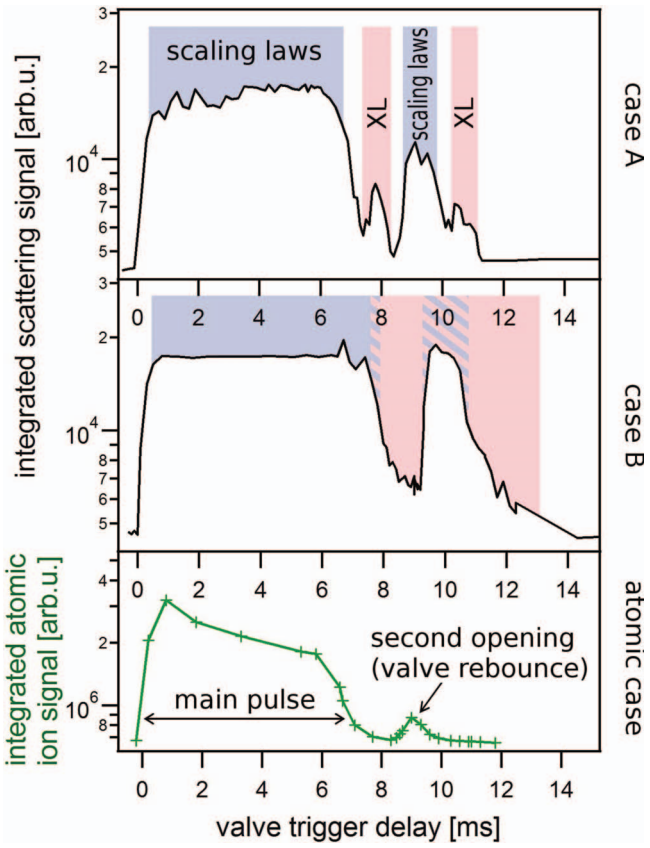

FIG. 6. Scans of the valve trigger delay in respect to the arrival time of the FEL-pulse. (a) Integrated scattering signal versus trigger delay for case A. (b) Integrated scattering signal versus trigger delay for case B. (c) Integrated ion time-of-flight signal versus trigger delay for an atomic gas jet. See text for further explanation.

clarify the question of the origin of the large clusters after the closing of the valve: both after-pulses in the uppermost panel of Figure 6, of the long plateau and of the short rebounce, are very short and appear approximately half a millisecond after the first and second closing. It can therefore be excluded that the after-pulses of large clusters are a mere effect of *velocity slip*,[23] the mechanism that large clusters fly slower and are outpaced by smaller clusters and gas, because then the after-pulses would differ in duration and position in respect to the time of closing. Instead we conclude that the process of the generation of large clusters is intertwined with the closing of the valve. Previous experiments in the literature[24] using Rayleigh scattering on pulsed jets also showed after-pulses. Shao-Hui and coworkers[24] interpreted their findings as small seed-clusters from a pre-expansion in the small volume in front of the nozzle throat resulting in the growth of large clusters. We agree that the generation mechanism is specific to the pulsed valve and the used nozzle geometry, but instead we propose the following mechanism: The closing valve causes an additional compression of the gas in the small volume in front of the nozzle which shifts the expansion conditions towards more extreme values and subsequently leads to the formation of large clusters. Further measurements and computational modeling will be necessary to ultimately answer this question.

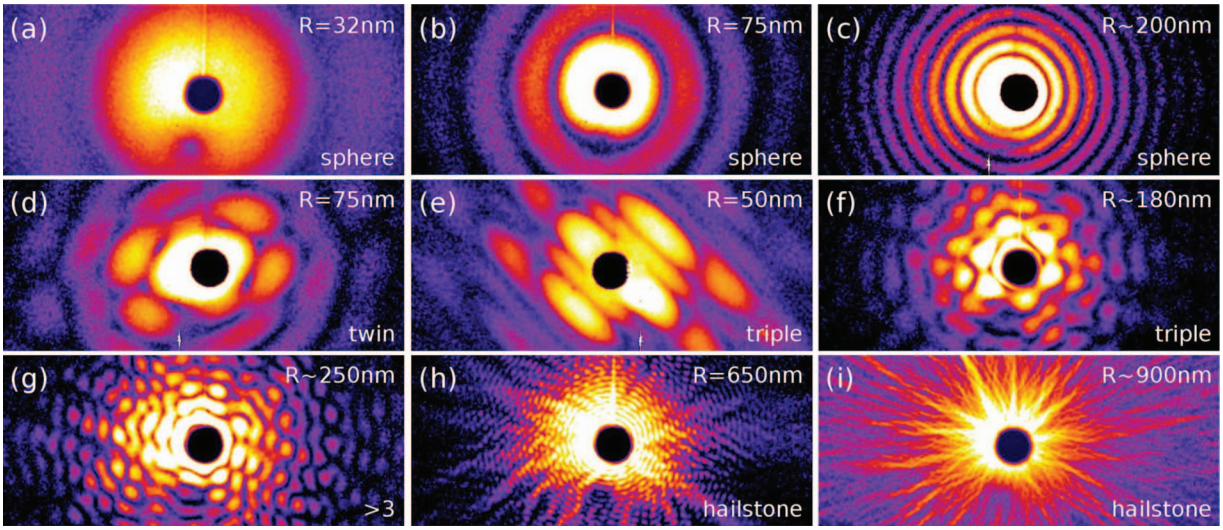

FIG. 7. Examples for single-cluster scattering patterns. The typical shape of clusters changes with increasing size from spherical over twin and triple structures to grainy hailstones.

V. GRAINY SUBSTRUCTURE OF GIANT CLUSTERS

The information on the shape of the clusters contained in the scattering patterns can be used to gain further insight into the growth mechanisms in a gas expansion. Coagulation is known to be the leading growth process for larger clusters,[25,26] and not monomer addition which is dominant in the initial growth period. However, the information whether the coagulating clusters reach spherical ground state, expected from energetic considerations, or freeze out in an intermediate non-spherical state was not accessible with previous methods, because it is not possible to deposit rare-gas clusters on a substrate.

Representative examples of single cluster scattering patterns from xenon clusters with radii between 32 nm and approximately 1 μm are displayed in Figure 7. Up to radii of 200 nm, spherical clusters such as in Figs. 7(a)–7(c) have been found coexisting with non-spherical structures. For cluster sizes around 50 nm radius we observe about 20% twin and even very seldom triple structures such as the patterns displayed in Figures 7(d) and 7(e). A more quantitative analysis of this size range has been published previously.[17] Towards larger sizes, non-spherical shapes such as in Figures 7(f)–7(i) become more abundant; from 300 nm radius on we did not observe any smooth ring patterns. In some cases the symmetry of the scattering pattern suggests a number of clusters sticking together such as observed in Fig. 7(f), where a threefold symmetry can be assumed. But with increasing size the structures tend to become more and more complicated (cf. Figs. 7(g)–7(i)). For clusters larger than 700 nm radius such as the example displayed in Figure 7(i) only a rough estimate of $r \sim 1\ \mu$m can be given.

It would be very desirable to reconstruct the 3D cluster shape from the scattering patterns and attempts to that goal using phase retrieval algorithms and 3D simulation methods are ongoing. However, iterative phase retrieval[27] has turned out to be difficult in particular in case of the larger clusters mainly because of the missing information in the center of the scattering patterns.

But already simple simulations as displayed in Figure 8 based on 2D Fourier transformed outlines can give an idea of the underlying cluster shape, even though only twin and triple structures can be assumed to be good matches. The simulations support an overall tendency for clusters around 50 nm to freeze out in intermediate non-spherical shapes

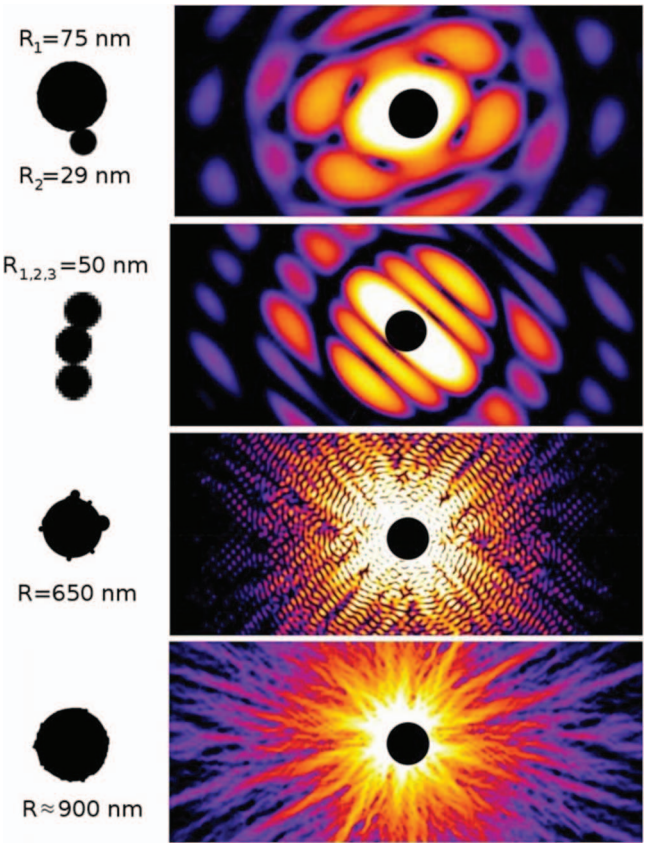

FIG. 8. Simple simulations of characteristic structures in the scattering patterns in Figs. 7(d), 7(e), 7(h), and 7(i). 2D projections in the left column are used for calculating patterns via 2D FFT, which are displayed in the right column.

during coagulation (Figs. 7(d) and 7(e)), continuing towards larger sizes up to μm-sized hailstone-like, mostly spherical particles with a grainy substructure (Figs. 7(h) and 7(i)). An open question and subject to future studies is the temperature dependency of the cluster shape and the ability to return to spherical ground state. Another interesting aspect in this context would be studying the generation and structure of mixed clusters,[28–30] which are especially interesting for the investigation of electron-ion recombination.

VI. SUMMARY AND OUTLOOK

In summary we have shown with single-particle imaging techniques that the time structure of pulsed cluster jets shows a large variation in produced cluster sizes. Long after the main pulse is over, extremely large clusters are produced exceeding the prediction from scaling laws by multiple orders of magnitude. The generation of large clusters in the after pulse is attributed to the closing poppet in the pulsed valve which leads to additional compression of the gas. In addition to the cluster size, the single particle images of the clusters reveal fine structure connected to the cluster morphology. Clusters up to approximately 100 nm appear mostly spherical with a significant fraction of twinned clusters. For larger clusters of several hundreds of nanometers radius, hailstone-like structures are most abundant. Their grainy shape indicates that the particles which grow by coagulation tend to freeze in non-spherical intermediate structures from a certain grain size on. The discovery and characterization of these giant clusters gives access to a new regime of studies on laser-cluster interaction ranging from infrared to x-rays.

ACKNOWLEDGMENTS

We want to acknowledge the excellent support from IOAP and DESY workshops. The first author is thankful for DAAD funding and helpful discussions with Ken Ferguson (SLAC). M.M. and T.G acknowledge funding from Leibnitz Graduate School *DinL* and the Ewald Fellowship of Volkswagen Stiftung for research with ultrafast x-ray sources. The work has been funded by BMBF Grant No. 05K10KT2/05K13KT2 and DFG Grant No. BO 3169/2-2.

[1]T. Ditmire, T. Donnelly, A. Rubenchik, R. Falcone, and M. Perry, Phys. Rev. A **53**, 3379 (1996).
[2]H. Wabnitz, L. Bittner, A. R. B. de Castro, R. Döhrmann, P. Gürtler, T. Laarmann, W. Laasch, J. Schulz, A. Swiderski, K. von Haeften, T. Möller, B. Faatz, A. Fateev, J. Feldhaus, C. Gerth, U. Hahn, E. Saldin, E. Schneidmiller, K. Sytchev, K. Tiedtke, R. Treusch, and M. Yurkov, Nature (London) **420**, 482 (2002).
[3]T. Fennel, K.-H. Meiwes-Broer, J. Tiggesbäumker, P.-G. Reinhard, P. Dinh, and E. Suraud, Rev. Mod. Phys. **82**, 1793 (2010).
[4]C. Bostedt, M. Adolph, E. Eremina, M. Hoener, D. Rupp, S. Schorb, H. Thomas, A. R. B. de Castro, and T. Möller, J. Phys. B **43**, 194011 (2010).
[5]C. Bostedt, E. Eremina, D. Rupp, M. Adolph, H. Thomas, M. Hoener, A. R. B. de Castro, J. Tiggesbäumker, K.-H. Meiwes-Broer, T. Laarmann, H. Wabnitz, E. Plönjes, R. Treusch, J. Schneider, and T. Möller, Phys. Rev. Lett. **108**, 093401 (2012).
[6]T. Gorkhover, M. Adolph, D. Rupp, S. Schorb, S. Epp, B. Erk, L. Foucar, R. Hartmann, N. Kimmel, K.-U. Kühnel, D. Rolles, B. Rudek, A. Rudenko, R. Andritschke, A. Aquila, J. Bozek, N. Coppola, T. Erke, F. Filsinger, M. Gorke, H. Graafsma, L. Gumprecht, G. Hauser, S. Herrmann, H. Hirsemann, A. Hömke, P. Holl, C. Kaiser, F. Krasniqi, J.-H. Meyer, M. Matysek, M. Messerschmidt, D. Miessner, B. Nilsson, D. Pietschner, G. Potdevin, C. Reich, G. Schaller, C. Schmidt, F. Schopper, C. Schröter, J. Schulz, H. Soltau, G. Weidenspointer, I. Schlichting, L. Strüder, J. Ullrich, T. Möller, and C. Bostedt, Phys. Rev. Lett. **108**, 245005 (2012).
[7]S. Schorb, D. Rupp, M. Swiggers, R. Coffee, M. Messerschmidt, G. Williams, J. Bozek, S.-I. Wada, O. Kornilov, T. Möller, and C. Bostedt, Phys. Rev. Lett. **108**, 233401 (2012).
[8]O. Hagena, Surf. Sci. **106**, 101 (1981).
[9]O. Hagena, Rev. Sci. Instrum. **63**, 2374 (1992).
[10]R. Karnbach, M. Joppien, J. Stapelfeld, J. Wörner, and T. Möller, Rev. Sci. Instrum. **64**, 2838 (1993).
[11]U. Buck and R. Krohne, J. Chem. Phys. **105**, 5408 (1996).
[12]F. Dorchies, F. Blasco, T. Caillaud, J. Stevefelt, C. Stenz, A. Boldarev, and V. Gasilov, Phys. Rev. A **68**, 023201 (2003).
[13]W. Ackermann, G. Asova, V. Ayvazyan, A. Azima, N. Baboi, J. Bähr, V. Balandin, B. Beutner, A. Brandt, A. Bolzmann *et al.*, Nat. Photon. **1**, 336 (2007).
[14]General Parker Valve, 99 series.
[15]K. Tiedtke, A. Azima, N. von Bargen, L. Bittner, S. Bonfigt, S. Düsterer, B. Faatz, U. Frühling, M. Gensch, C. Gerth, N. Guerassimova, U. Hahn, T. Hans, M. Hesse, K. Honkavaar, U. Jastrow, P. Juranic, S. Kapitzki, B. Keitel, T. Kracht, M. Kuhlmann, W. B. Li, T. Martins, M. Nunez, E. Plönjes, H. Redlin, E. Saldin, E. Schneidmiller, J. Schneider, S. Schreiber, N. Stojanovic, F. Tavella, S. Toleikis, R. Treusch, H. Weigelt, M. Wellhöfer, H. Wabnitz, M. Yurkov, and J. Feldhaus, New J. Phys. **11**, 023029 (2009).
[16]H. Thomas, C. Bostedt, M. Hoener, E. Eremina, H. Wabnitz, T. Laarmann, E. Plönjes, R. Treusch, A. R. B. de Castro, and T. Möller, J. Phys. B **42**, 134018 (2009).
[17]D. Rupp, M. Adolph, T. Gorkhover, S. Schorb, D. Wolter, R. Hartmann, N. Kimmel, C. Reich, T. Feigl, A. R. B. de Castro, R. Treusch, L. Strüder, and T. Möller, New J. Phys. **14**, 055016 (2012).
[18]In this area of the scattering detector background signal from stray-light and ions was minimal.
[19]See http://encyclopedia.airliquide.com/encyclopedia.asp for Air Liquide online data base.
[20]It is not clear whether the xenon in case D (Fig. 3) is in a liquid or oversaturated gaseous state.
[21]G. Chen, B. Kim, B. Ahn, and D. Kim, J. Appl. Phys. **106**, 053507 (2009).
[22]As atomic ions produce a very low scattering signal, this cannot be used to trace the time structure of a gas jet. On the other hand, the atomic ion signal can be considered proportional to the number of atoms in the interaction region. This is not the case for cluster ions which have kinetic energy and therefore are transmitted differently through the time-of-flight spectrometer.
[23]S. Khmel and R. Sharafutdinov, J. Tech. Phys. **43**, 986 (1998).
[24]L. Shao-Hui, L. Bing-Chen, N. Guo-Quan, and X. Zhi-Zhan, Chin. Phys. **12**, 856 (2003).
[25]J. Soler, N. Garcia, O. Echt, K. Sattler, and E. Recknagel, Phys. Rev. Lett. **49**, 1857 (1982).
[26]R. Jansen, I. Wysong, S. Gimelshein, M. Zeifmann, and U. Buck, J. Chem. Phys. **132**, 244105 (2010).
[27]S. Marchesini, H. He, H. Chapman, S. Hau-Riege, A. Noy, M. R. Howells, U. Weierstall, and J. Spence, Phys. Rev. B **68**, 140101(R) (2003).
[28]M. Lengen, M. Joppien, R. Müller, J. Wörner, and T. Möller, Phys. Rev. Lett. **68**, 2362 (1992).
[29]M. Hoener, C. Bostedt, H. Thomas, L. Landt, E. Eremina, H. Wabnitz, T. Laarmann, A. R. B. de Castro, and T. Möller, J. Phys. B **41**, 181001 (2008).
[30]L. Schroedter, M. Müller, A. Kickermann, A. Prystawik, S. Toleikis, M. Adolph, L. Flückinger, T. Gorkhover, L. Nösel, M. Krikunova, T. Oelze, Y. Ovcharenko, D. Rupp, M. Sauppe, D. Wolter, S. Schorb, C. Bostedt, T. Möller, and T. Laarmann, Phys. Rev. Lett. **112**, 183401 (2014).